

Application of Fluorescent Micro Particles as Geothermal Tracers

Hakki AYDIN, Serhat AKIN, Mustafa SALAR

Hakki.Aydin@metu.edu.tr, Serhat@metu.edu.tr, msalar@metu.edu.tr

Middle East Technical University, Ankara, Turkey

Keywords: Tracer, micro particles, rhodamine B, melamine resin

ABSTRACT

Tracer testing of flow between injection and production wells is an effective tool to map fluid flow pathways in a geothermal reservoir. Tracer concentration curves can be used to provide insight into projected thermal drawdown in the reservoir or thermal breakthrough of re-injected fluids, estimating inter-well volumes and flow geometries. Although radioactive tracers have been used in the past many tracer tests now use chemical tracers that are less hazardous to handle. Fluorescent organic compounds such as fluorescein and rhodamine-B, other fluorescent compounds such as naphthalene sulfonates and dissolved inorganic solutes such as potassium iodide (KI) and potassium bromide can be used as geothermal tracers. Nano-colloids have been suggested as ‘smart’ geothermal tracers. Tracer experiments were conducted using micro melamine resin rhodamine B particles with differing sizes ranging from 4 μm to 10 μm and conventional rhodamine B in a 2-D cross sectional model built from marble blocks that represents a low enthalpy liquid dominated geothermal reservoir. It has been observed that first arrival time of micro tracers was 4 times smaller than those observed in conventional rhodamine B tracer. The effect of injection rate, particle size and fracture geometry on micro particles was also investigated.

1. INTRODUCTION

In geothermal reservoir management, tracers have become an important tool for evaluating the nature of fracture system. Tracer study is an important technique for reservoir characterization, particularly in such specialized areas as geothermal engineering (Akin and Okandan, 1995). It provides a good insight to detect the short circulation of waste water between reinjection and production wells (Fossum and Horne, 1982). Conventional tracers that dissolve in water have been used widely and successfully in geothermal fields for understanding fracture connectivity because of their economic, stability at reservoir conditions and ease of detecting at extremely low concentrations. Although conventional tracers can provide a wide range of information about flow paths such as dispersivity, fluid velocity, pecclet number etc. with developed flow models, however they are still insufficient for detailed evaluation of transport system of the fractured rock. For example, it is difficult to evaluate the fracture aperture or matrix pore size with conventional tracer. In addition, conventional tracers have a high tendency of diffusion into rock matrix, which causes high retention. However, micro particles are very useful because of their physical and chemical controlling properties. Therefore, nanoparticle and micro particles have been introduced to overcome the restrictions with conventional tracers in fractured rocks. Several studies have been published regarding the application of particle tracers in fractured rocks. Zhang et al. (2015) investigated DNA-tagged nanotracer, which were coated with silica nanoparticles for applicability in geothermal reservoirs. They observed that silica nanoparticles showed good flow characteristics at high temperatures through porous media and these nanotracer were found to be viable for geothermal tracer applications. Rose et al. (2011), introduced colloidal nanocrystal quantum dots for quantitatively measuring the surface area of fractures within a geothermal and EGS reservoir. They stated that the potential of modifying surface chemistry and diameter of quantum dots can be used as a tool for characterizing fracture surface areas. In this study, the transport of micro melamine resin rhodamine B-marked particles is investigated in a 2-D cross sectional low enthalpy geothermal reservoir model built from marble blocks. The flow models of conventional rhodamine B and micro melamine particles are studied to find out similarities between the tracers and differences between them. We were also able to observe the recovery and retention of micro particles by controlling parameters such as particle size and injection rate.

2. MATERIALS AND METHODS

A low temperature geothermal reservoir model was built from 25 marble blocks with block dimensions of 5x10x10 cm (Figure 2) and fracture porosity of the system is calculated as 9.4 %. Another system was built with the same concept except that 50 marble blocks were used with block dimensions of 5x5x10 cm (Figure 1) and the fracture porosity of this system is calculated as 10.5%. The total bulk volume of the two systems is the same which is 13750 cc. The models were designed in such a way that the tracer was injected as a slug from the left bottom corner of the reservoir and samples were collected from the upper right corner of the system in 1 minute time intervals. The models represent a low enthalpy geothermal reservoir that produce from the shallower depth of a production well and inject into the deeper depth of an injection well. The experiments were conducted at the rates of 5cc/min, 15 cc/min, 30 cc/min and 45 cc/min for different particle sizes ranging from 4 μm to 10 μm . While continuous water injection, temperature and pressure were recorded in the several parts of the system.

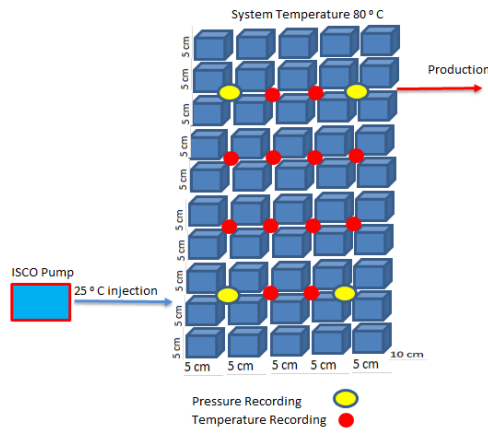


Figure 1: Model-A which consists from 5x5x10 cm dimensions of marble

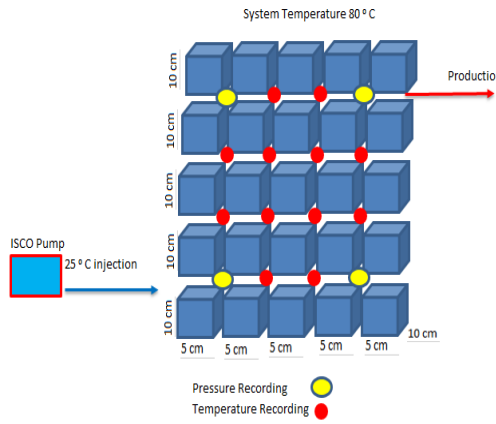


Figure 2: Model-B which consists from 5x10x10 cm dimensions of marble

Micro particles based on melamine resin, rhodamine B-marked, products were purchased from Sigma-Aldrich. Melamine resin microspheres are manufactured by acid-catalyzed hydrothermal polycondensation of methylol melamine in the temperature range of 70 to 100°C without any surfactants (Biofiles, 2007). Sigma Aldrich Inc. states that density of microsphere particles is 1.51 g/cm³, the particles are stable at temperature up to 300°C and they are stable in acids and bases. Surface of the particles is hydrophilic. The size and shape of the melamine resin particles were scanned using a polarizing transmitted light microscope (Figure 3). The particles are labelled with fluorescent dye of red color.

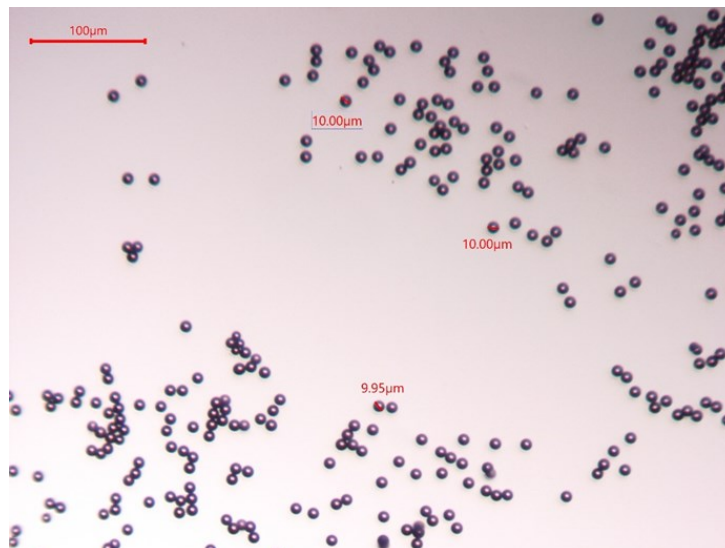


Figure 3: The size and shape of the melamine resin particles

The concentration of effluent was measured by using Turner Quantech Fluorimeter. The calibration run of the fluorimeter was conducted at different concentrations (i.e 0.25, 0.5, 1.0, 5.0, 75, 150 ppb). The regression constant of the calibration line was larger than 0.95 and the calibration was repeated at the beginning of the each experiment.

3. RESULTS AND DISCUSSIONS

The objective of the study is to investigate the applicability of the micro melamine resin as a tracer in geothermal reservoirs. The controlling parameters of the experiments were injection rate, particle size and fracture geometry. The Sigma Inc. gives the guarantee of the stability of melamine resin particles up to 300°C. Thus, the temperature of the experiments was not included in the controlling parameters and the temperature of the system was kept at 80°C.

Injection rate is a critical parameter impacting tracer recovery. In our experiments, as the injection rate was increased from 15 cc/min to 30 cc/min, the recovery of the 6 um particles increased from 0.84% to 12.35%. Similar results were obtained for 10 um and 4 um particles (Table 1). Similarly, Vilks and Bachinski (1996), found that below the critical velocity significant retention of particles was observed due to gravity settlement. The density of the micro melamine resin particles is 1.51 g/cm³, which is higher than water density. Therefore, it was found that in order to minimize gravity related particle settlement, the injection rate should be larger than 15 cc/min.

The recovery of the micro tracers was decreased as the particle size increased. Significant particles trapping was experienced for 4 um, 6 um and 10 um particles in the system that consisted of 5x5x10 cm blocks. Coagulated particles up to a length of 66 um were observed (Figure-4). There was no identifiable peak concentration due to particle trapping in the small fractures and the concentration of particles fell below the measurement limits in a short time (Figure 11, Figure 12, and Figure 13). However, when the same experiments were conducted in the system that consisted 5x10x10 cm blocks, it was observed that the recovery of the particles was significantly improved (Table 2). This indicates that the fracture aperture and particle size are the key parameters that limit the recovery of the particles.

Another purpose of the study is to find out the similarities and differences between conventional rhodamine B and micro melamine resin particles. Therefore, the tracer return curves of the micro tracers and conventional rhodamine-B were matched with the flow models that are described in Akin (2001). By minimizing the sum of the square differences, multi-fracture model was best matched with tracer experiment data (Figure 6). Once a good match was obtained, reservoir model parameters were then determined corresponding equations. It was found that the Peclet numbers were higher than 1 for all the tracers, which corresponded to an advection dominant system. Rhodamine B tracer return curves dispersion was smaller compared to micro melamine resin particles. This suggests that conventional rhodamine B may not find time to leave the high conductive channels and enter several fractures. However, since the density of micro particles are higher than water, there may be a chance for micro particles to enter more fractures compare to rhodamine B. It was also observed that first arrival time of melamine resin particles was 4 times less than that of conventional rhodamine-B. Similarly, Bales et al., (1989) reported that the transport of bacteriophages in fractured porous tuff was three times faster than conventional tracer.

By using moment analysis method (Shook and Forsmann, 2005), tracer return curves were analyzed. Figure 14 shows the flow-storage capacity of the micro particles and rhodamine B. It was observed that rhodamine B is closer to 45° line (homogeneous fractures) compared to micro particles and 4 um particle size is closer to rhodamine-B. Lorentz coefficient and the Dkystra-Parsons coefficient are two different measures of heterogeneity that are used to quantify the reservoir flow path heterogeneity (Lake, 1989). As it is mentioned in Shook and Forsmann, Lorentz coefficient varies between 0 and 1. The larger the Lorentz coefficient value, the more heterogeneous the flow paths are. In our experiments, Lorentz coefficient increases with increasing particle size. Rhodamine-B has the smallest Lorentz coefficient, which means it is homogeneous compared to micro particles. Dkystra-Parsons coefficient values are similar for the micro particles, however rhodamine-B has different flow paths (Table-5). Figure 15 shows a plot of interstitial velocity and storage capacity. The curves of micro particles have an inflection at the same point but with a different magnitude of interstitial velocity. This means that micro tracers travel through the same paths, however due to transport mechanisms the magnitudes of the interstitial velocity are not the same. Rhodamine-B has an interstitial velocity somewhat smaller than that of the micro particles, however they become identical as the storage capacity increases. It was also observed that interstitial velocity at the production side is several orders higher than average the average velocity of the tracers presented in Table 4. This suggests that as the drainage distance of the production point increases the velocity of the flow decreases.

4. CONCLUSIONS

Microsphere melamine resin particles have been successfully used as a micro tracers to identify connection of fractures in a low enthalpy experimental geothermal reservoir model. It was found that the recovery of the micro particles increased with increasing flow rate. However, the rates of the test should be high enough to prevent particle trapping in fracture media. The particle size has an inverse relation with particle recovery. Tracer return curve and flow characteristic of 4 um particle (the smallest one) was similar to conventional rhodamine-B. The first arrival of the micro particles was 4 times sooner than that of the conventional rhodamine B. It was concluded that physical controlling of the micro particles is an important property that can be used to characterize fractures.

REFERENCES

1. Akin, S.: Analysis of tracer tests with simple spreadsheet models. *Computer and Geosciences*, March 2001.
2. Akin, S., Okandan, E.: Reservoir characterization by tracer testing. *Proceedings of the World Geothermal Congress*, Florence, Italy, Vol. 2, pp. 1145-1150, 1995.
3. Bales, R.C., Gerba, C.P., Grondin, G.H., and Jensen, S.L.: Bacteriophage Transport in Sandy Soil and Fractured Tuff. *Appl. Environ. Microbiol.*, 55, 2061-2067, (1989).
4. Fossum, M.P., Horne, R.N.: Interpretation of tracer return profiles at Wairakei geothermal field using fracture analysis, *Geothermal Resources Council Transactions* 6, 261-264, (1982).

5. Lake, L.W.: Enhanced Oil Recovery, Englewood Cliffs, New Jersey, Prentice Hall, (1989).
6. Rose, P., Riasetto, D., Siy, Jacqueline., Bartl, M., Reimus, P., Mella, M., Leecaster, K., and Petty, S.: Quantum Dots As Tracers in Geothermal and EGS Reservoirs. *Proceedings, Thirty-Sixth Workshop on Geothermal Reservoir Engineering*, Stanford University, (2011).
7. Shook, G.M., Ansley, S.L., Wylie, A.: Tracers and Tracer Testing: Design, Implementation, and Interpretation Methods. Idaho Water Resource Research Institute, University of Idaho, (2004).
8. Vilks, P., Bachinski, D.B.: Particle and suspended particle migration experiments in a granite fracture. *Journal of Contaminant Hydrology* 21, 269-279, (1996).
9. Zhang, Yuran., Manley, T.S., Li, K., Horne, R.N.: DNA-Encapsulated Silica Nanoparticles Tracers for Fracture Characterization, *Geothermal Resources Council Transactions*, Vol.39, (2015).

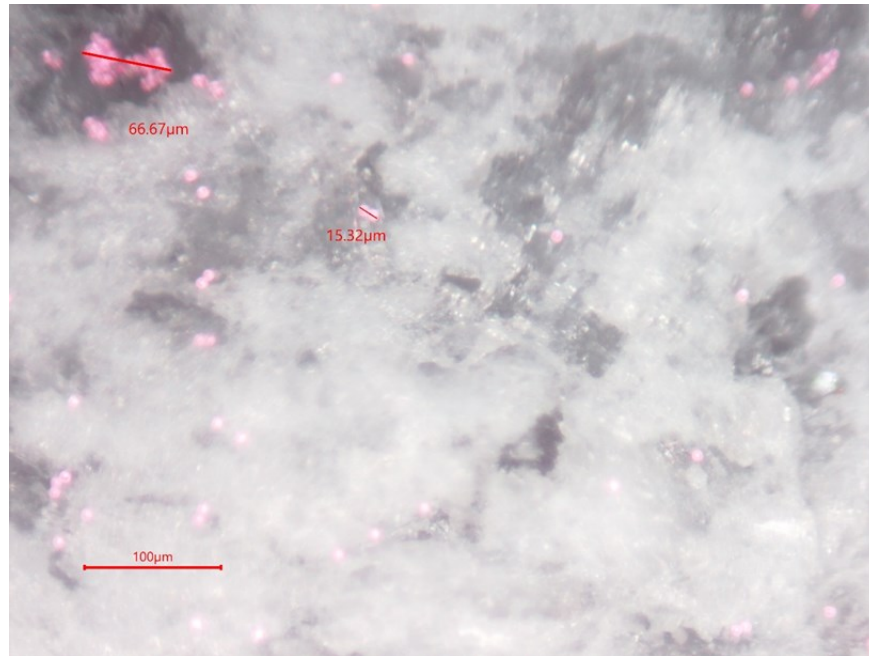


Figure 4: Agreement of the melamine resin particles

Dimension of Blocks 5x5x10cm				
size(um)	rate(cc/min)	Recovery (%)	First arrival time(min)	mean arrival time(min)
4	15	2.62	1.36	NA
6	15	0.84	1.36	NA
6	30	12.35	0.68	NA
10	15	1.67	1.36	NA
10	45	3.57	0.45	NA

Table 1: Recovery of particles in 5x5x10 cm block dimensions

Dimension of Blocks 5x10x10				
size(um)	rate(cc/min)	Recovery (%)	First arrival time(min)	mean arrival time(min)
4	15	38.71	1.5	102.35
6	15	21.49	2	97.30
10	15	17.5	2	82.00

Table 2: Recovery of particles in 5x10x10 cm block dimensions

Rhodamine-B Dimension of Blocks 5x10x10				
Concentration (ppm)	Rate (cc/min)	Recovery (%)	First arrival time (min)	mean arrival time (min)
10	5	52.93	29	258
10	15	98.54	9.5	102.7

Table 3: Recovery of conventional rhodamine B in 5x10x10 cm block dimensions

Tracers	Pe	J	tm(min)	e	m(ug)	DL(cm ² min ⁻¹)	u(cm min ⁻¹)
Rhodamine-B 15 cc/min	24.7	538.80	38.0	0.4701	34	1.5	0.98
	2.40	208005	164.0	0.0009	180	3.5	0.23
	7.80	437.9	76.0	0.520	80	2.4	0.50
um 15 cc/min	8.07	7.96	135.9	0.5314	1.85	1.28	0.28
	3.17	17065.4	49.0	0.00016	1.15	9.06	0.77
	1.44	1.85	11.6	0.4668	0.26	84.17	3.23
6 um 15 cc/min	5.35	2.76	160	0.551	0.89	1.64	0.23
	3.72	14796	51.44	0.00013	0.77	7.35	0.73
	1.38	1.29	15.26	0.4484	0.20	66.78	2.46
10 um 15 cc/min	4.68	1.49	117.31	0.5745	0.46	2.56	0.32
	2.86	14105	50.20	0.00007	0.44	9.80	0.75
	1.55	0.99	12.54	0.42344	0.13	72.53	2.99

Table 4: Results of Multi-fracture Model

	Lorenz Coefficient	Dykstra-Parsons Coefficient	Mean Residence Time (min)	Pore Volume cm3
Rhodamine-B	0.281	0.290	102.7	1440
4 um particle	0.356	0.334	102.35	465.9
6 um particle	0.376	0.335	97.3	307
10 um particle	0.381	0.393	82	210

Table 5: Heterogeneity of tracers

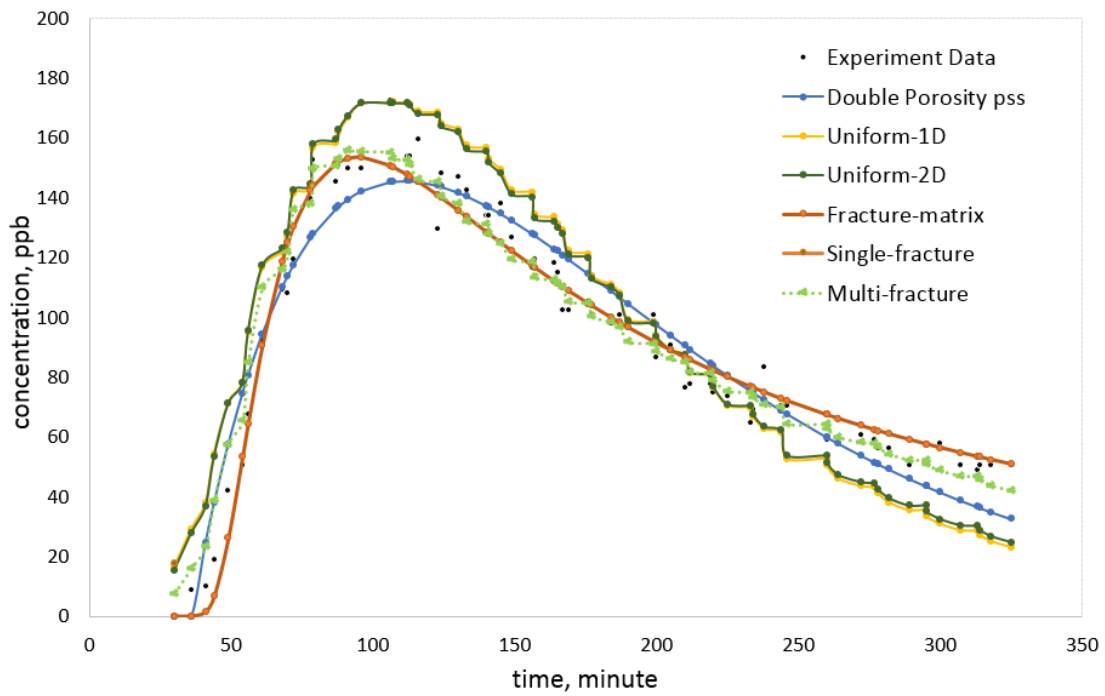


Figure 5: Comparison of models to experiment rhodamine-B return curve at 5 cc/min

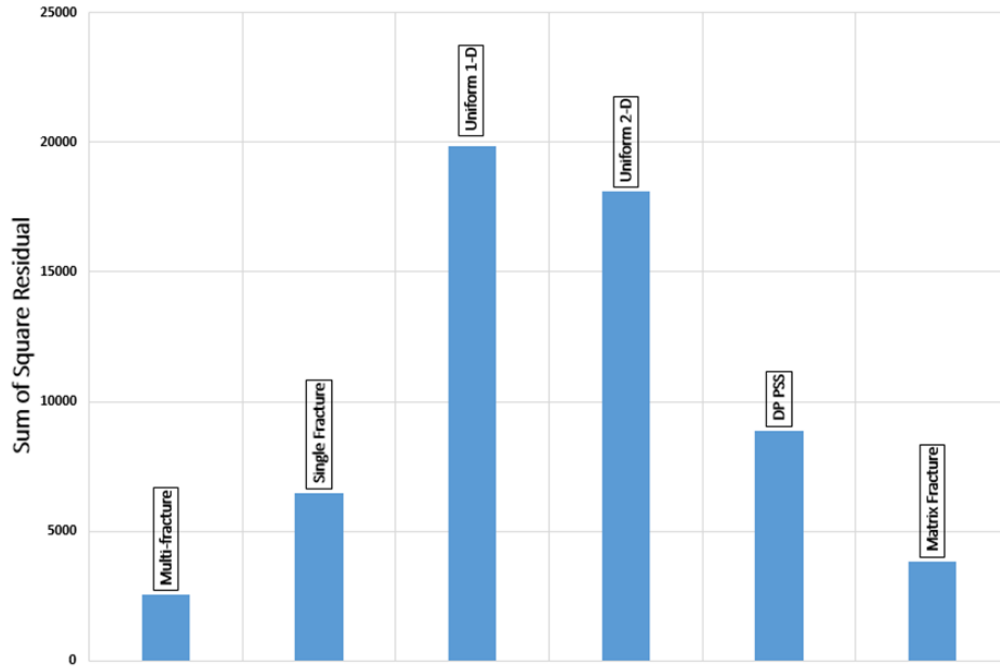


Figure 6: Sum of squares residual for different models

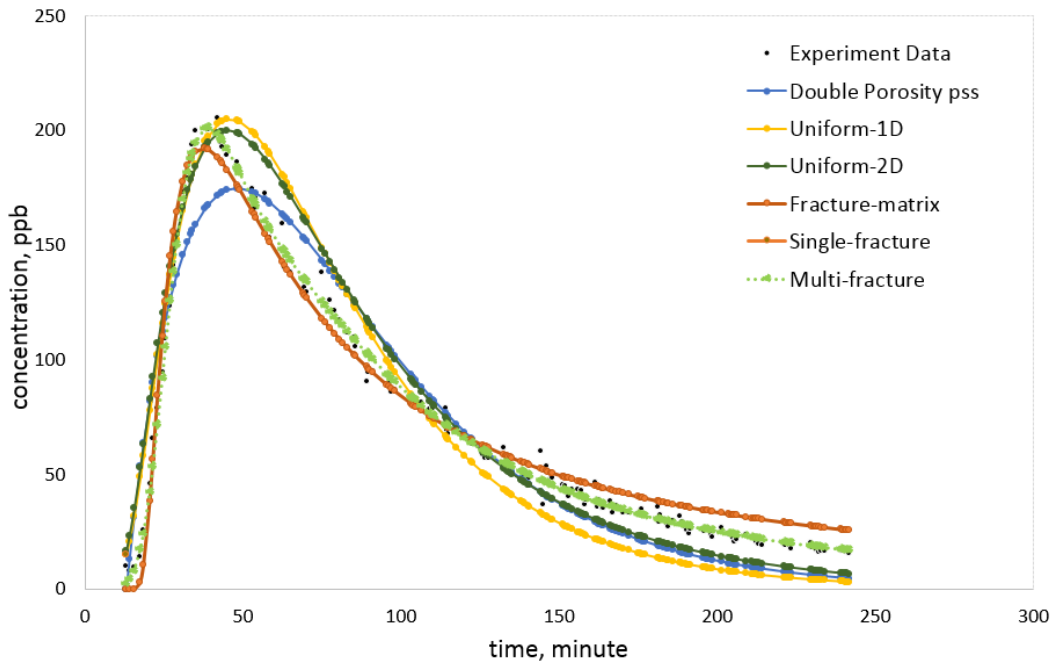


Figure 7: Comparison of models to experiment rhodamine-B in 5x10x10 cm dimensions return curve at 15 cc/min

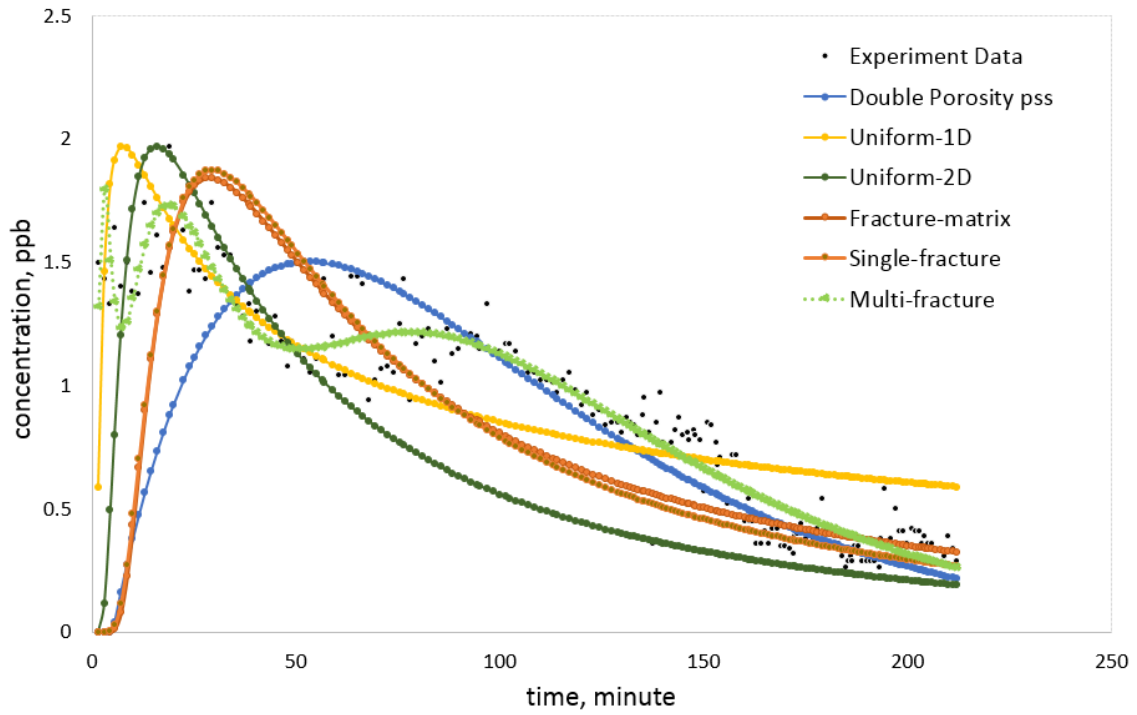


Figure 8 Comparison of models to experiment 4 um particle in 5x10x10 cm dimensions return curve at 15 cc/min

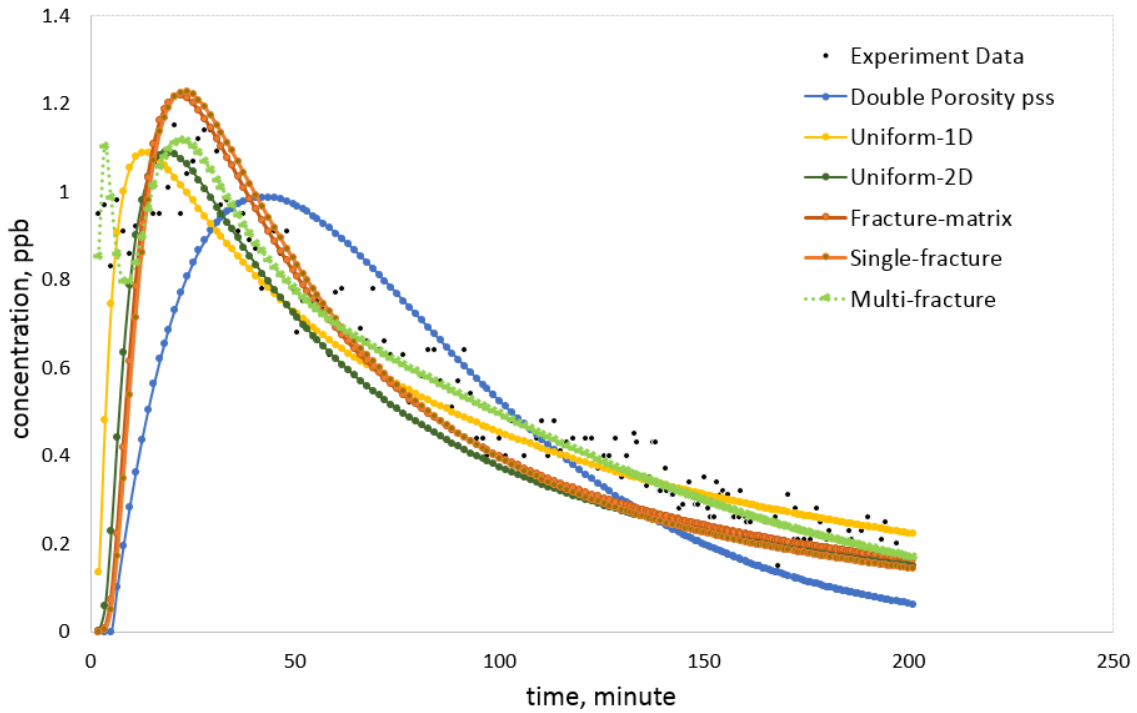


Figure 9 Comparison of models to experiment 6 um particle in 5x10x10 cm dimensions return curve at 15 cc/min

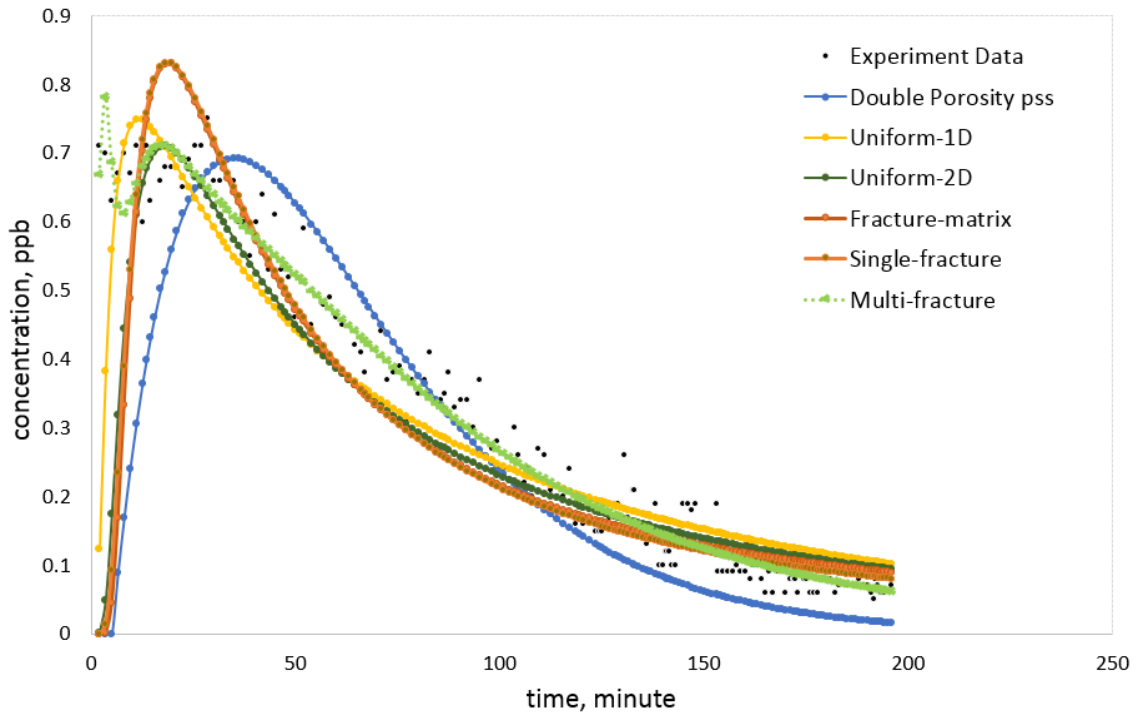


Figure 10 Comparison of models to experiment 10 um particle in 5x10x10 cm dimensions return curve at 15 cc/min

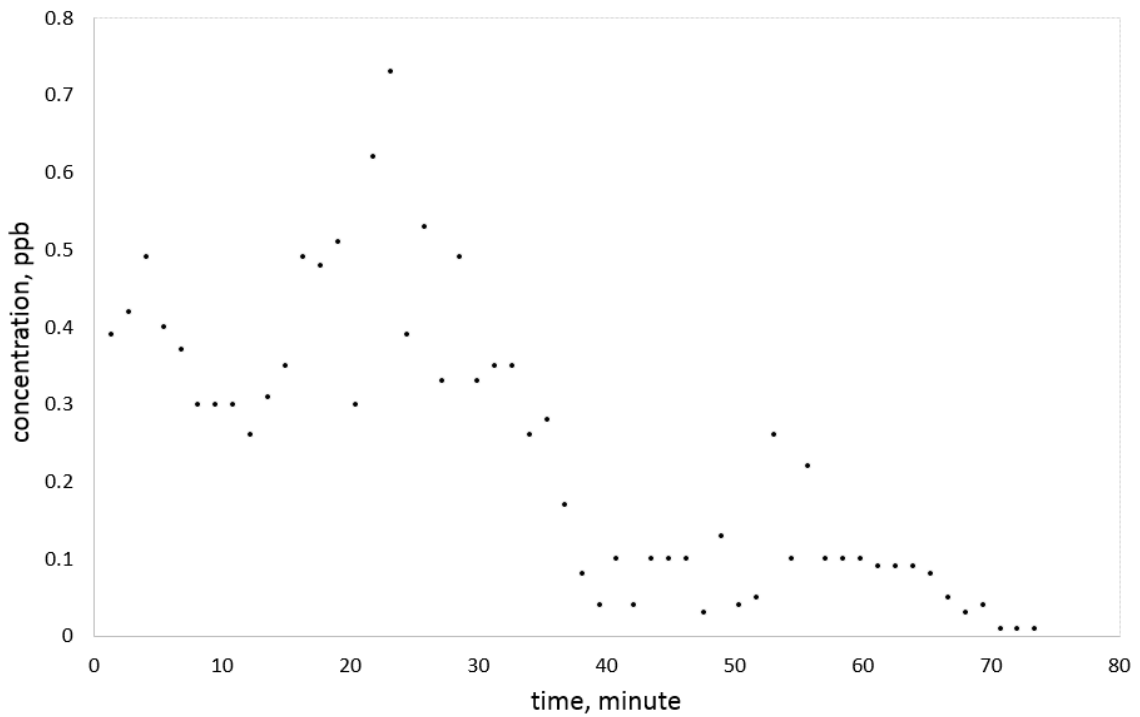


Figure 11: Tracer return curve of 4 um particle in 5x5x10 cm dimensions of blocks

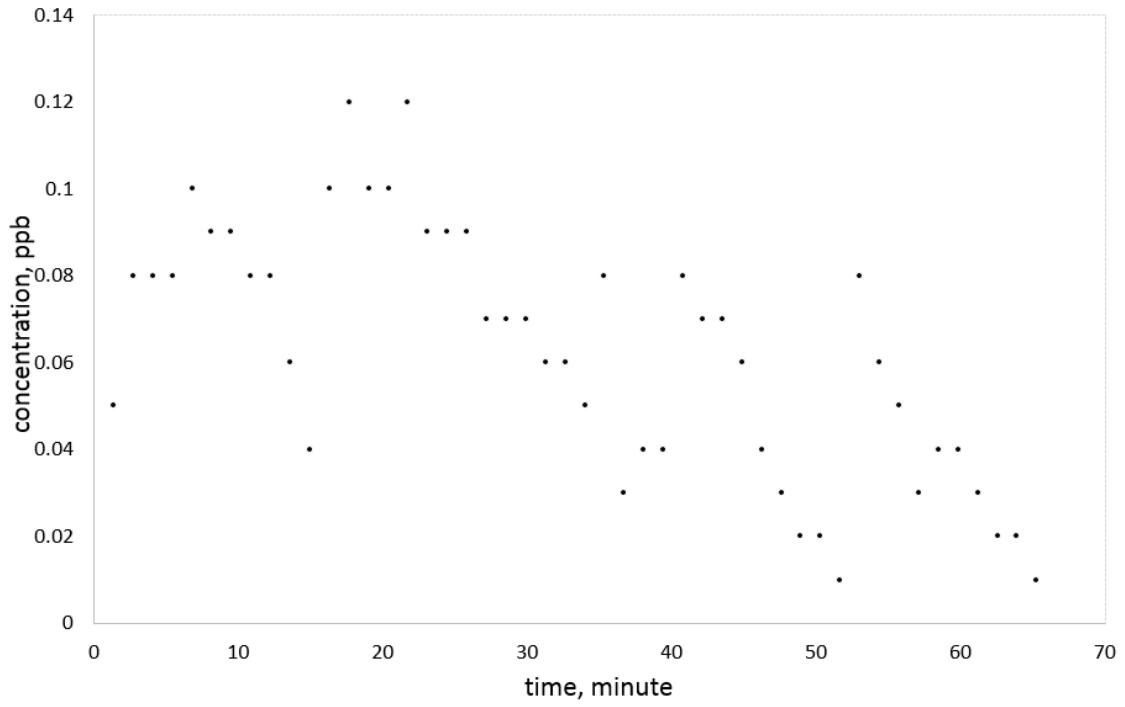


Figure 12: Tracer return curve of 6 um particle in 5x5x10 cm dimensions of blocks

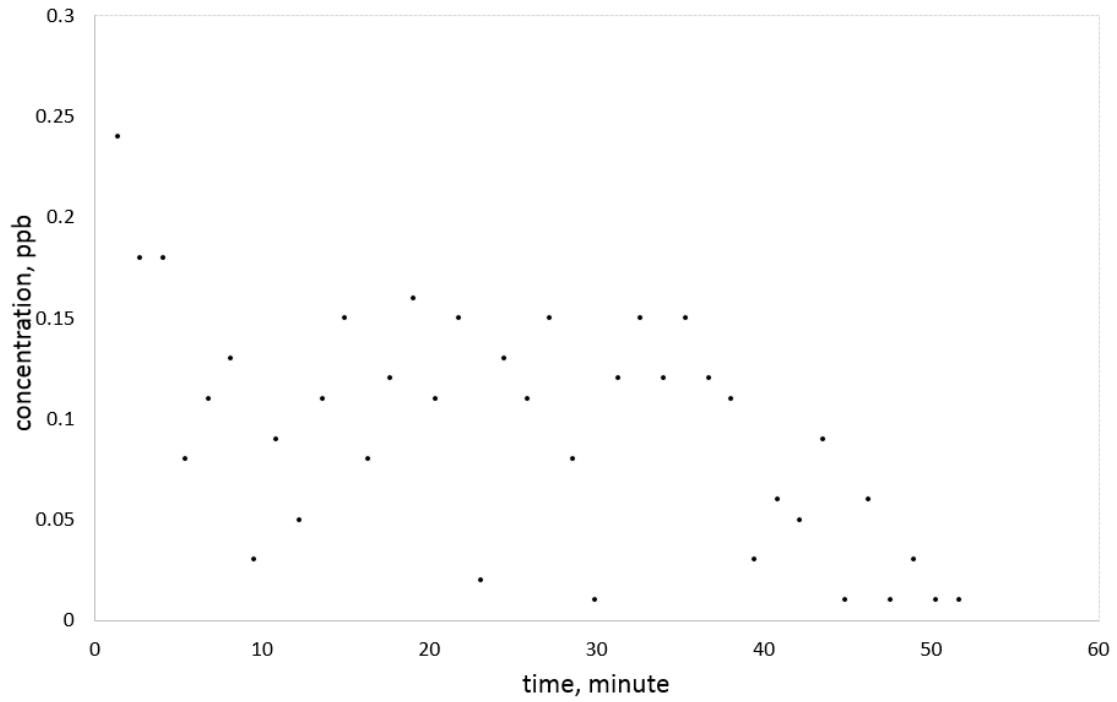


Figure 13: Tracer return curve of 10 um particle in 5x5x10 cm dimensions of blocks

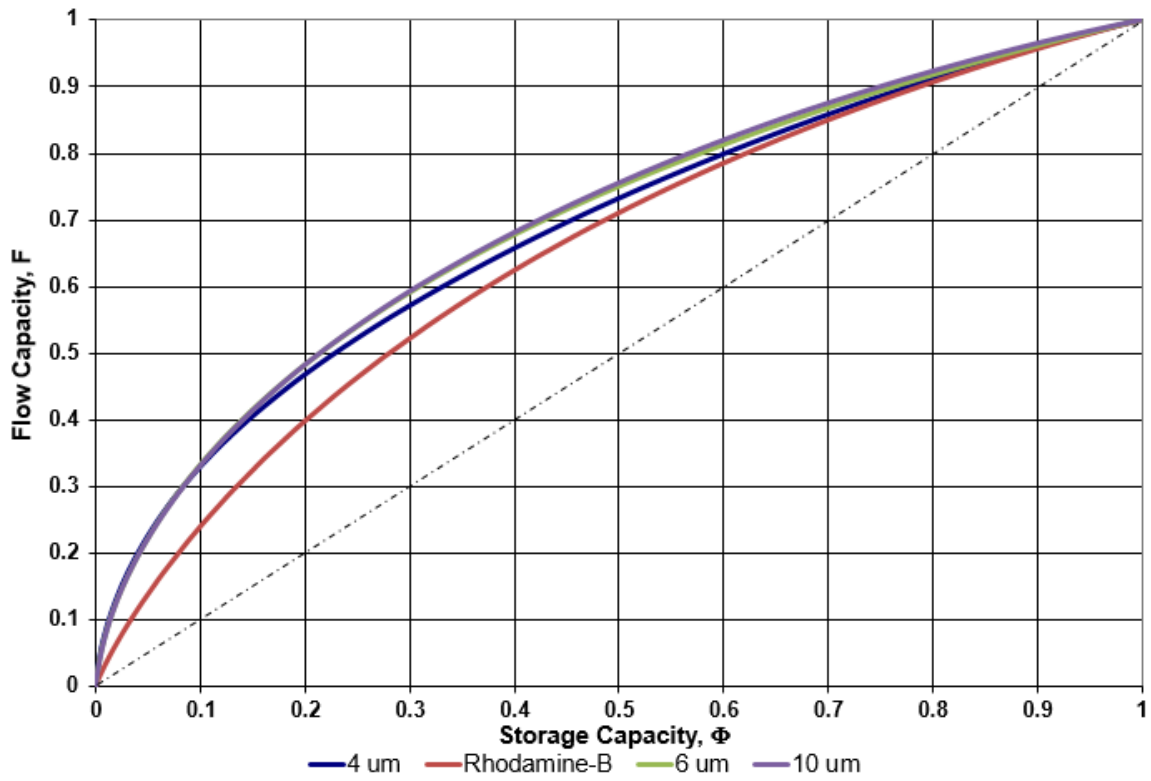


Figure 14: Flow geometry of the tracers in 5x10x10 cm dimensions of blocks

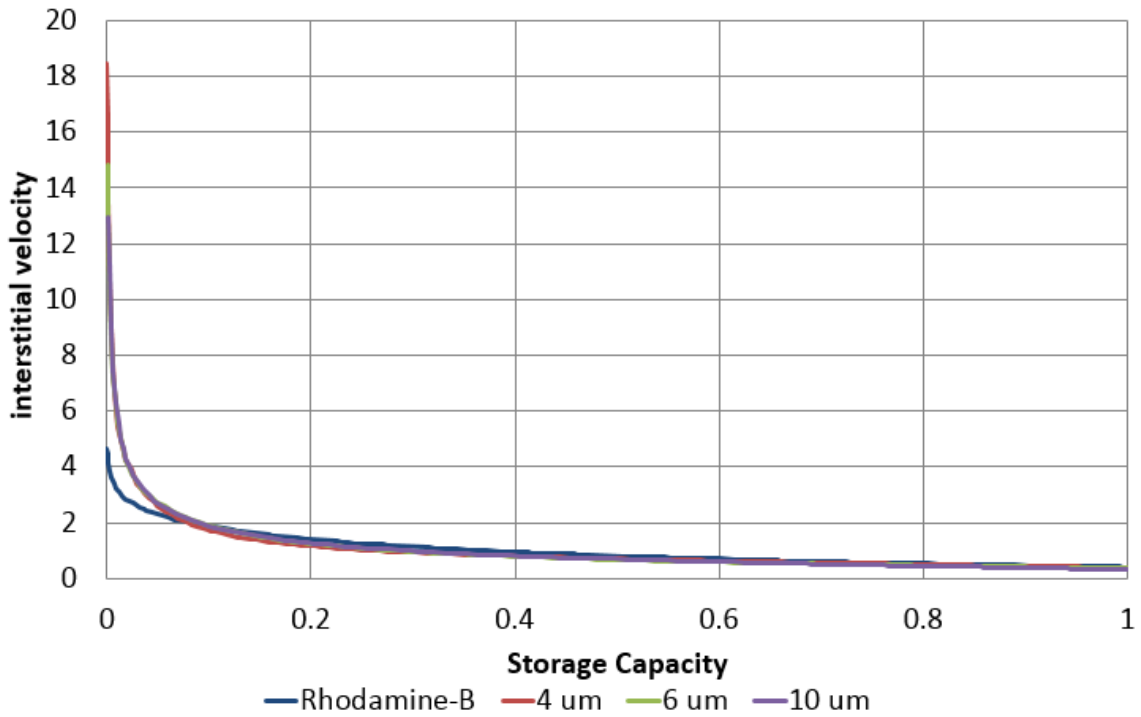


Figure 14: Interstitial velocity of the tracers in 5x10x10 cm dimensions of blocks